Enhancing fiber/matrix bonding in polypropylene fiber reinforced cementitious composites by microbially induced calcite precipitation pre-treatment

[1,2]Yifei HAO, [3,4]Liang CHENG*, [5]Hong HAO and [6]Mohamed A SHAHIN

Yifei HAO: [1]State Key Laboratory of Hydraulic Engineering Simulation and Safety, Tianjin University, Tianjin, China; [2]School of Civil Engineering, Tianjin University, Tianjin, China. Email: hao.yifei@tju.edu.cn

Liang CHENG: [3]Biofules Institute of Jiangsu University, Jiangsu University, Jiangsu, China; [4]School of Civil and Environmental Engineering, Nanyang Technological University, Singapore. Email: Lcheng@ntu.edu.sg

Hong HAO: [5]Tianjin University and Curtin University Joint Research Center of Structural Monitoring and Protection, Centre for Infrastructural Monitoring and Protection, School of Civil and Mechanical Engineering, Curtin University, Kent Street, Bentley, WA 6102, Australia. Email: hong.hao@curtin.edu.au

Mohamed A SHAHIN: [6]Department of Civil Engineering, School of Civil and Mechanical Engineering, Curtin University, Kent Street, Bentley, WA 6102, Australia. M.Shahin@curtin.edu.au

* Corresponding author. Email: lcheng@ntu.edu.sg

Abstract

In fiber reinforced cementitious composites (FRCC), bonding between the fibers and matrix governs many important properties, including strengths, fracture energy, ductility, and energy absorption capacities. This study explores the application of a microbiological process of microbially induced calcite precipitation (MICP) to pre-treating surface of polypropylene (PP) fibers for enhancing the interfacial boning strength. This technique utilizes MICP process to produce calcium carbonate that binds onto the fiber surface, leading to increased interfacial bond area and strength. Laboratory tests indicate that MICP modification could increase the post-cracking resistance and energy absorption capacity of the FRCC beam specimens by 58% and 69.3%, respectively. Microstructure analysis reveals that PP fibers after MICP treatment were coated with a layer of $CaCO_3$ with thickness around 20-50 μm depending on the degree of deposition. Results acknowledged a significant role of MICP pre-treatment in enhancing the fiber-matrix bonding properties of FRCC and the corresponding mechanical performance.

Keywords: Microbially Induced Calcite Precipitation; Mechanical Properties; Fiber Reinforcement; $CaCO_3$

1. Introduction

Cementitious materials are relatively brittle, with tensile strengths that are typically only about one tenth of their corresponding compressive strengths. To overcome such disadvantage, for many applications, it is becoming increasingly popular to reinforce the cementitious matrix with small, randomly distributed fibers, named fiber-reinforced cementitious composites (FRCC) for crack control. These fibers provide micro- to meso-scale reinforcement for reduced shrinkage cracking and spreading, as well as prevention and control of initiation, propagation, and coalescence of cracks [1]. Polypropylene (PP) fibers are popular for reinforcing cementitious composites due to their unique properties such as high melting point, chemical stability, and relatively low cost compared to other types of fibers. However, polypropylene is typically hydrophobic, resulting in poor bonds with cementitious matrices [2]. Furthermore, PP fibers have low surface free energy and very smooth surface structures that may be susceptible to slipping or de-bonding from the cementitious matrix.

To date, various approaches of surface treatment have been employed to improve the efficiency of PP fibers in the cementitious composites on the basis of physical, chemical and mechanical methods to enhance the fiber-matrix adhesion [3-5]. For example, Denes et al. [6] applied $SiCl_4$ plasma-activated PP fibers to FRCC, resulting in better flexural strength and toughness due to the effective improvement of compatibility between the hydrophobic fiber and hydrophilic cementitious matrix. Lovato and Fahmy [7] demonstrated that the increase in wettability of the surface of PP fibers after chemical treatment contributed to an improvement of the compressive strength of FRCC. Di Maida et al. [8] used sol-gel technique to coat nano-silica particles onto the surface of PP fibers, leading to remarkable improvement in the bonding energy and

maximum load by 239% and 120%, respectively. However, this process is not cost-effective as several expensive chemicals, such as tetraethyl-orthosilicate, are needed.

It is known that calcium carbonate ($CaCO_3$) crystals are well compatible with cement matrix [9]. By depositing $CaCO_3$ crystals onto the surface of PP fibers, the mechanical properties of FRCC may be improved due to the increased roughness of PP fibers surface and the enhanced interfacial bonding between fibers and matrix. Microbially induced calcite precipitation (MICP) through urea hydrolysis pathway, an emerging research subject in recent years, has been used to enhance the durability of structural materials by forming a protective calcite layer on the surface [10] or acting as healing material in the surficial cracks [9]. Choi et al. [11] demonstrated an extensive calcite crystal precipitation, in addition to the effective bonding between the microbially induced calcite and cement matrix, on the surface of polyvinyl alcohol fibers through MICP treatment. In the current study, the feasibility of using MICP for the surface modification of the PP fibers is investigated for the first time, and the corresponding mechanical properties of FRCC using MICP modified PP fibers are examined through a series of laboratory tests.

2. Experimental programme

2.1 Mortar matrix and PP fibers

The mortar matrix used in this study was prepared by mixing water, cement and sand with a mass ratio of 1:2:4. The 28-day uniaxial compressive strength of the matrix was determined by testing 50 mm cubes according to the ASTM C109-13 standard [12]. Six cubes were tested, and the averaged uniaxial compressive strength was found to be 37.73 MPa with standard deviation of 2.37 MPa. The PP fibers used in the current study had a rectangular cross section of 1.5×0.7 mm^2, and their mechanical properties are given in Table 1.

79 **Table 1.** Mechanical properties of PP fibers

Tensile strength	Young's modulus	Maximum tensile strain
500 MPa	8 GPa	8%

80

81 *2.2 Microorganisms and cementation solution*

82 The urease active bacteria used in the current study were *Bacillus sp.* strain (DSM 23526) [13],
83 which were cultivated in an aerobic batch growth medium as reported in a previous study by
84 Cheng and Shahin [14]. The optical density (OD_{600}) of the harvested culture varied between 3
85 and 3.15, and the urease activity was approximately 15 U/mL (1U is equal to 1μmol of urea
86 hydrolyzed per minute). The culture was stored in a 4°C refrigerator for not more than 1 week
87 prior to use. The cementation solution used consisted of 1 M of calcium chloride (111 g/L) and
88 1 M of urea (60 g/L).

89

90 *2.3 MICP pre-treatment of PP fibers*

91 The process of MICP pre-treatment of PP fibers was conducted by submerging the fibers into
92 a biological reagent solution, a mixture of bacterial culture and cementation solution, as stated
93 in the Section 2.2, using a volume ratio of 1:1, for 24 hours to allow for the MICP to deposit
94 and coat the fiber surface. The volume ratio between the added fibers and biological reagent
95 solution was about 1:4. The fibers with different amount of coating (i.e. minor, moderate, and
96 heavy), which was calculated using the net dry weight increase of the fibers after the coating
97 divided by the initial weight of the untreated fibers, were prepared through repeated treatment
98 with the biological reagent solution.

99

100 *2.4 Tests conducted*

101 In the present study, systematic tests were carried out on a series of corroboration for the
102 effectiveness of MICP pre-treatment on enhancing the reinforcing effects of PP fibers in the
103 cementitious matrix. The characteristics of the $CaCO_3$ coating layer on the surface of PP fibers
104 were examined using scanning electron microscopy (SEM) after the MICP pre-treatment. The
105 properties of the fiber/matrix interfacial bonding were then characterized by carrying out a
106 number of single fiber pull-out tests. The force-slip relations were recorded and compared so
107 that the modification level of MICP pre-treatment which gave the best effects could be
108 determined. Furthermore, a number of mid-point bending tests on beam specimens reinforced
109 with PP fibers with an optimal level of MICP modification determined from the fiber pull-out
110 tests were performed. The force-displacement relations were recorded and compared for
111 evaluation. In addition, uniaxial compressive tests on FRCC cylinders with treated and
112 untreated PP fibers were carried out to examine the influence of MICP pre-treatment on the
113 compressive strength since it is one of the key parameters in design of concrete structures. SEM
114 and energy-dispersive X-ray (EDX) analyses were also conducted on the pre-treated and
115 untreated fibers, after the bending tests, to confirm the microstructure and the corresponding
116 mechanism. The test results and observations are presented below.
117

118 **3. Results and discussions**

119 *3.1 Pre-test SEM analyses*

120 The PP fibers were grouped as REF (without MICP modification), A (with minor deposition，
121 0.026 g $CaCO_3$/g fiber), B (with moderate deposition, 0.094 $CaCO_3$ g/g fiber) and C (with
122 heavy deposition, 0.372 $CaCO_3$ g/g fiber). The unit of $CaCO_3$ g/g fiber was defined as the
123 average amount of $CaCO_3$ (grams) precipitated on one gram of fiber. The treated and untreated

PP fibers were shown in Fig. 1a. Coating materials on the surface of the PP fiber can be visualized clearly. It is interesting to note that after the pretreatment by scraping the fiber with tightly pinched fingernails, micro fiber strings were found to peel off from the macro one, suggesting that the bonding strength between the coating layer and the macro PP fiber should be higher than that among the micro fibers (Fig. 1b). The SEMs of the MICP modified PP fibers, namely groups A, B and C, are shown and compared in Fig. 2. As can be seen, when the fibers were treated once with the biological reagents (Group A, Fig. 2a & b), a very small amount of $CaCO_3$ was coated onto the fibers' surface, which may have a negligible contribution to enhancing the fiber/matrix bonding properties. For Group B (Fig. 2c & d), the fibers' surface was partially covered by a layer of $CaCO_3$ crystals. It can be found that either individual crystals or coagulated crystal clusters that connect together forming a layer of calcite coating on the surface of the fiber (Fig. 2c & d). The thickness of the coating layer is estimated to be approximately equivalent to the size of the individual crystal or the crystal clusters, assuming the shape of these crystals are relatively spherical, which is about 20-50 μm. The roughening of the fibers' surface should be able to increase the contact area between the fiber and matrix, leading to enhancing both the anchorage bonding and frictional bonding. However, when the fibers were scanned (Group C, Fig. 2e & f), which were treated with several batches of biological reagent solution, it was found that the fibers were almost completely covered with the coating layer, as can be seen in Fig. 2e. Although the contact area was further increased compared to Group B, because of the brittleness of the $CaCO_3$ layer, it is expected that the coating might have low resistance and hence easily de-bond from the fibers during the fiber pull-out process, resulting in adverse effect for the fiber/matrix bonding enhancement. These hypotheses are further tested and proved by the following single fiber pull-out tests.

3.2 Single fiber pull-out tests

Individual PP fibers with different levels of MICP pre-treatment were placed in the matrix with an embedment depth of 30 mm, with its longitudinal direction normal to the specimen surface. The pull-out tests were carried out by pulling the individual fibers out of the matrix with a rate equal to 1mm/min. For each tested group, three samples were prepared and examined for less-biased results. The averaged force-slip relations obtained from the pull-out tests are shown in Fig. 3. It can be seen that in the initial stage of the fiber pull-out, the stiffness (slope) in the force-slip relation increases with the increase of the level of MICP modification. While Groups A and B had slightly higher stiffness than the unmodified fiber (Group REF), the stiffness was significantly increased for Group C. This can be attributed to the much higher contact area between the fiber, $CaCO_3$ and matrix due to the thick layer of coating, as shown in Fig. 2. As can be seen in Fig. 3b, compared to the reference samples, the very minor deposition in Group A did not improve the peak force but slightly enhanced the residual pull-out resistance. The peak resistance and energy absorption of Group B fibers were found to be 26.7% and 91.0%, respectively, higher than those obtained from Group REF. It is interesting to note that the very heavy deposition (Group C) even resulted in a slight reduction in the peak resistance and insignificant change in the post-peak resistance. This is consistent with the expectation according to the SEM analyses (Section 2) that the brittle $CaCO_3$ coating leads it to easily de-bonding from the fibers and loses its function. It should be noted that indeed, the main benefit induced by the calcite deposition process consists in the increase in the peak of the pullout force (for the Group B of fibers). However, a softening behavior is still observed during the extraction of the single fiber after the peak. Other kinds of treatment, like nano-silica deposition, although more expansive, induce an advantageous hardening behavior up to the complete fiber pullout, which may increase the energy required for the total fiber extraction of two or three times [8].

As the fibers of Group B outperform those of the other groups in the fiber pull-out tests in terms of the peak force, residual resistance and energy absorption capacity, they were used to prepare the PP FRCC specimens for the mid-point bending tests.

3.3 Mechanical properties of PP FRCC materials

To further examine the contribution of the MICP pre-treatment to the bending strength of FRCC materials, a number of mid-point bending tests were carried out on beam specimens casted with 1% by volume PP fibers from Group B (with moderate deposition) and Group REF (without MICP modification). The 37.5 mm long fibers were mixed with the mortar matrix and 74 × 74 × 285 mm cast specimens. Three specimens were prepared and tested for each batch. The loading rate was 1mm/min, and all tests were terminated when the vertical deflection reached 20 mm. The averaged force-deflection curves of the FRCC beams with and without MICP modification are compared, as shown in Fig. 4a. It can be seen that the general failure processes and force-deflection relations of the two batches are similar. When the specimens started to pick up the load, they quickly reached their peak resistance at similar deflection of around 0.7 mm, immediately after which the resistance suddenly dropped due to the cracking of the mortar matrix. The fibers were then activated to bridge the cracks and provided residual or post-cracking resistance to the bending and were subjected to pull-out process. The post-cracking resistance of the beam specimens increased to a second peak then gradually decreased following a trend consistent with the pull-out behavior of fibers as shown in Fig. 3. The averaged peak resistance of specimens from Groups REF and B were 6120.6 and 6658.4 N, respectively, indicating that the MICP modification slightly improved the bending strength or modulus of rupture (by only 8.8%). However, the modified fibers remarkably increased the post-cracking resistance from 2328.5 to 3679.7 N, with an increment of 58%. This may be attributed to the enhanced peak and residual resistance of fibers of moderate deposition to the

198 pull-out action. The energy absorption capacities up to the deflection of 20 mm were calculated
199 by integrating the force-deflection curves (see Fig. 4b). As can be seen, the MICP modification
200 increased the energy absorption of the FRCC specimen by about 69.3%.

201 In addition to the mid-point bending tests, a number of uniaxial compressive tests were also
202 conducted to examine the influence of MICP pre-treatment on the compressive strength of PP
203 FRCC materials. Cylindrical specimens with diameter 100 mm and height 200 mm were
204 prepared and tested according to the ASTM C39 of ASTM standards [15]. The average
205 compressive strength of FRCC for untreated PP fibers was 39.07 MPa, whereas that of FRCC
206 with PP fibers from Group B was 36.39 MPa, with a reduction of 6.86% compared to the former,
207 indicating the adverse effect of MICP pre-treatment on the compressive strength of PP FRCC
208 materials, but the reduction in the compressive strength is insignificant.

209 The slight reduction of compressive strength resulted from MICP pre-treatment might be
210 because of the additional calcite coating with relatively weaker mechanical property than the
211 matrix or the PP fiber as an additional phase in the composite. However, considering the minor
212 reduction of the compressive strength but the largely improved flexural response, the benefit
213 of introducing MICP pre-treatment on PP fibers to the mechanical properties of FRCC material
214 is marked.

215

216 *3.4 Post-test SEM and EDX analyses*

217 The SEM images for both the untreated and biochemical MICP treated PP fibers after the mid-
218 point bending tests are presented in Fig. 5, showing a notable difference in the degree of
219 abrasion between the treated (a, b) and untreated (c, d) fibers. Scratches caused by the pull-out
220 effect can be observed on the surface of both the treated and untreated samples. However, much
221 severer phenomena of PP strings peeling off from the fibers matrix was observed on the surface

of the treated fibers as a consequence of the likely increased chemical and mechanical bonding between the treated fibers and cement, compared to the untreated fibers. It was also found that some particles were bonded to the fibers after the fiber surface peeling off occurred.

The chemical composition of the residual micrometric particles was confirmed by EDX spectra. For the untreated fibers (Fig. 6a & b), the elements of Si, O and Ca shown in the EXD mapping image and the EDX spectrum (spot analysis) reveal the presence of various possible cement hydrated or carbonated products, such as C-S-H, $Ca(OH)_2$, and even $CaCO_3$. For the MICP treated fibers after the mid-point bending tests, the EDX mapping image and EDX spectrum (spot analysis) indicate that those crystals found between the peeled fibers strings (red rectangle area) are likely to be pure $CaCO_3$ crystals due to the very minor amount of Si present (Fig. 6c & d). The magnified image of these crystal clear indicates the imprints of the bacterial cells shape (holes) on the surface of crystals, suggesting the presence of bacteria produced $CaCO_3$ (MICP) [14] (Fig. 6e). It is also interesting to note that the $CaCO_3$ crystals found between the peeled fiber strings suggests a strong chemical and mechanical bonding.

4. Conclusions

This paper reports a series of laboratory tests to investigate the effects of MICP pre-treatment on the microstructural and mechanical properties of cementitious material reinforced with PP fibers. The SEM and EDX analyses indicated that MICP induced CaCO3 were successfully deposited on the surface of PP fibers. The fiber pull-out test demonstrated that the moderate deposition of CaCO3 coating in MICP modification level of about 0.094 CaCO3/g fibers yielded the best improved fiber/matrix bonding properties. Through mid-point bending tests, it was demonstrated that the MICP modification could increase the post-cracking resistance and

energy absorption capacity of FRCC beam specimens by about 58% and 69%, respectively. The feasibility and effectiveness of MICP pre-treatment for enhancing the bonding between PP fibers and cementitious material were proven.

Acknowledgement

The first author acknowledges the support from National Natural Science Foundation of China under grant no.: 51778415. The authors would like to thank the financial support from Australian Research Council.

References

[1] L. Vandewalle, Post cracking behaviour of hybrid steel fiber reinforced concrete, Proc., 6th Int. Conf. on Fracture Mechanics ofConcrete and Concrete Structures—FraMCoS-6, Catania, Italy, 2007, Vol. 3, pp 1367–1375.

[2] Z. Zheng, D. Feldman, Synthetic fiber-reinforced concrete, Prog. Polym. Sci. 20 (1995) 185–210.

[3] M. Pei, D. Wang, Y. Zhao, X. Hu, Y. Xu, J. Wu, D. Xu, Surface treatments of subdenier monofilament polypropylene fibers to optimize their reinforcing efficiency in cementitious composites, J. Appl. Polym. Sci. 92 (2004) 2637-2641.

[4] Q.F. Wei, Surface characterization of plasma-treated polypropylene fibers, Mater. Charact. 52(2004) 231-235.

[5] B. Felekoglu, K. Tosun, B. Baradan, A comparative study on the flexural performance of plasma treated polypropylene fiber reinforced cementitious composites, J. Mater. Process. Technol. 209 (2009) 5133-5144.

[6] F. Denes, D. Feldman, Z.Q. Hua, Z. Zheng, R.A. Young, Cementitious-matrix composites from $SiCl_4$-plasma-activated polypropylene fibers, J Adhes. Sci. Technol. 10 (1996) 61-77.

[7] N.L. Lovata, M.F. Fahmy, Interfacial bond study of a chemically treated polypropylene fiber-reinforced concrete, Constr. Build. Mater. 1(1987) 83-87.

[8] P. Di Maida, E. Radi, C. Sciancalepore, F. Bondioli, Pullout behavior of polypropylene macro-synthetic fibers treated with nano-silica. Constr. Build. Mater. 82 (2015) 39–44.

[9] J.Y. Wang, D. Snoeck, S. Van Vlierberghe, W. Verstraete, N. De Belie, Application of hydrogel encapsulated carbonate precipitating bacteria for approaching a realistic self-healing concrete, Constr. Build. Mater. 68 (2014) 110-119.

[10] C.X. Qian, J.Y. Wang, R.X. Wang, L. Cheng, Corrosion protection of cement-based building materials by surface deposition of CaCO3 by Bacillus pasteurii, Mater. Sci. Eng. C 29 (2009) 1273-1280.

[11] S.G. Choi, K. Wang, J. Chu, Properties of biocemented, fiber reinforced sand, Constr. Build. Mater. 120 (2016) 623-629.

[12] ASTM C109 / C109M-16a, Standard Test Method for Compressive Strength of Hydraulic Cement Mortars (Using 2-in. or [50-mm] Cube Specimens), ASTM International, West Conshohocken, PA, 2016.

[13] S. Al-Thawadi, R. Cord-Ruwisch, Calcium carbonate crystals formation by ureolytic bacteria isolated from Australian soil and sludge, J. Adv. Sci. Eng. Res. 2 (2012) 12–26.

[14] L. Cheng, M. Shahin, Urease active bio-slurry: a novel soil improvement approach based on microbially induced carbonate precipitation, Can. Geotech. J. 53 (2016) 1-10.

[15] ASTM C39 / C39M-17a, Standard Test Method for Compressive Strength of Cylindrical Concrete Specimens, ASTM International, West Conshohocken, PA, 2017.

293 **Caption**

294 **Fig. 1.** Images of PP fibers (a) treated and untreated with MICP, (b) after scarped with tightly
295 pinched fingernails.

296 **Fig. 2.** SEM of MICP modified PP fiber with (a) minor deposition (0.026 g $CaCO_3$/g fiber); (c)
297 moderate deposition (0.094 $CaCO_3$ g/g fiber); and (e) heavy deposition (0.372 $CaCO_3$ g/g fiber).
298 (b), (d), and (f) are the magnified images of the red circle area indicated on the (a), (c) and (e)
299 images, receptively.

300 **Fig. 3.** Comparison of force-slip relations in the pull-out tests: (a) x-scale (0-3 mm), y-scale
301 (0-100 N); and (b) full scale.

302 **Fig. 4**. Comparison of the performance of fiber reinforced mortar beams under mid-point
303 bending (a) force-deflection relations and (b) energy absorption capacities.

304 **Fig. 5.** SEM images of untreated (a, b) and treated (c, d) PP fibers taken after the mid-point
305 bending tests. (b) and (d) are the magnified images of the red rectangle area indicated on the
306 (a) and (c) images, receptively.

307 **Fig. 6.** EDX spectrums of deposits on the surface of untreated (a, b), MICP treated PP fibers
308 (c, d) after the mid-point bending tests, and (e) magnified image of the red rectangle area
309 indicated on the (c) image.

310

Figure 1

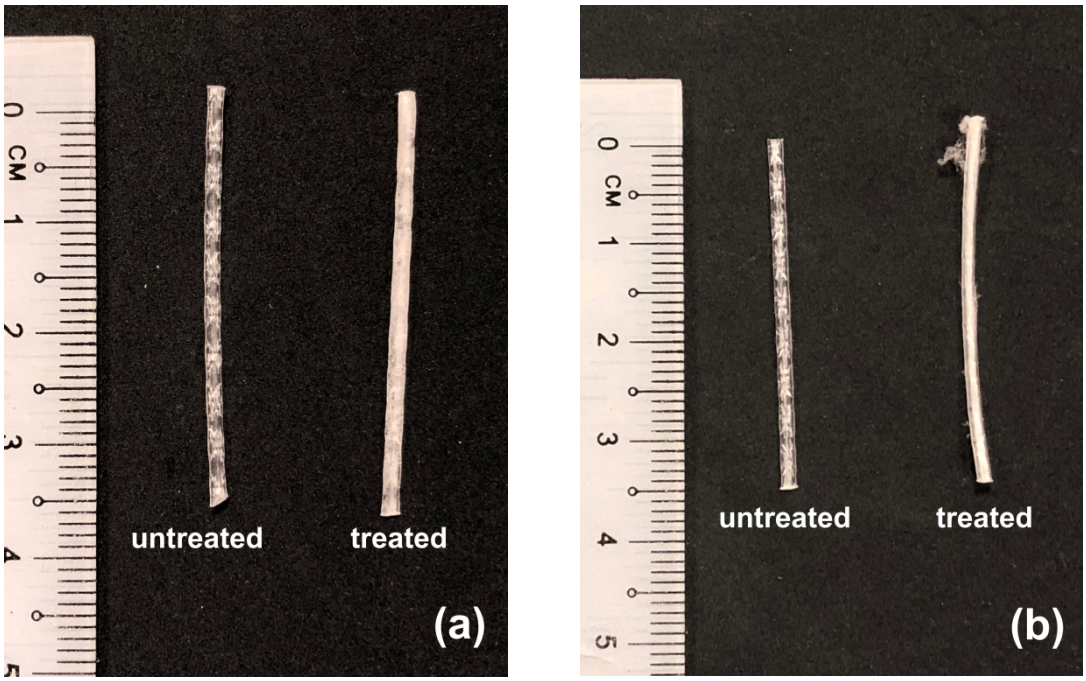
0 CM 1 2 3 4 5
untreated
treated
(a)
0 CM 1 2 3 4 5
untreated
treated
(b)

Figure 2

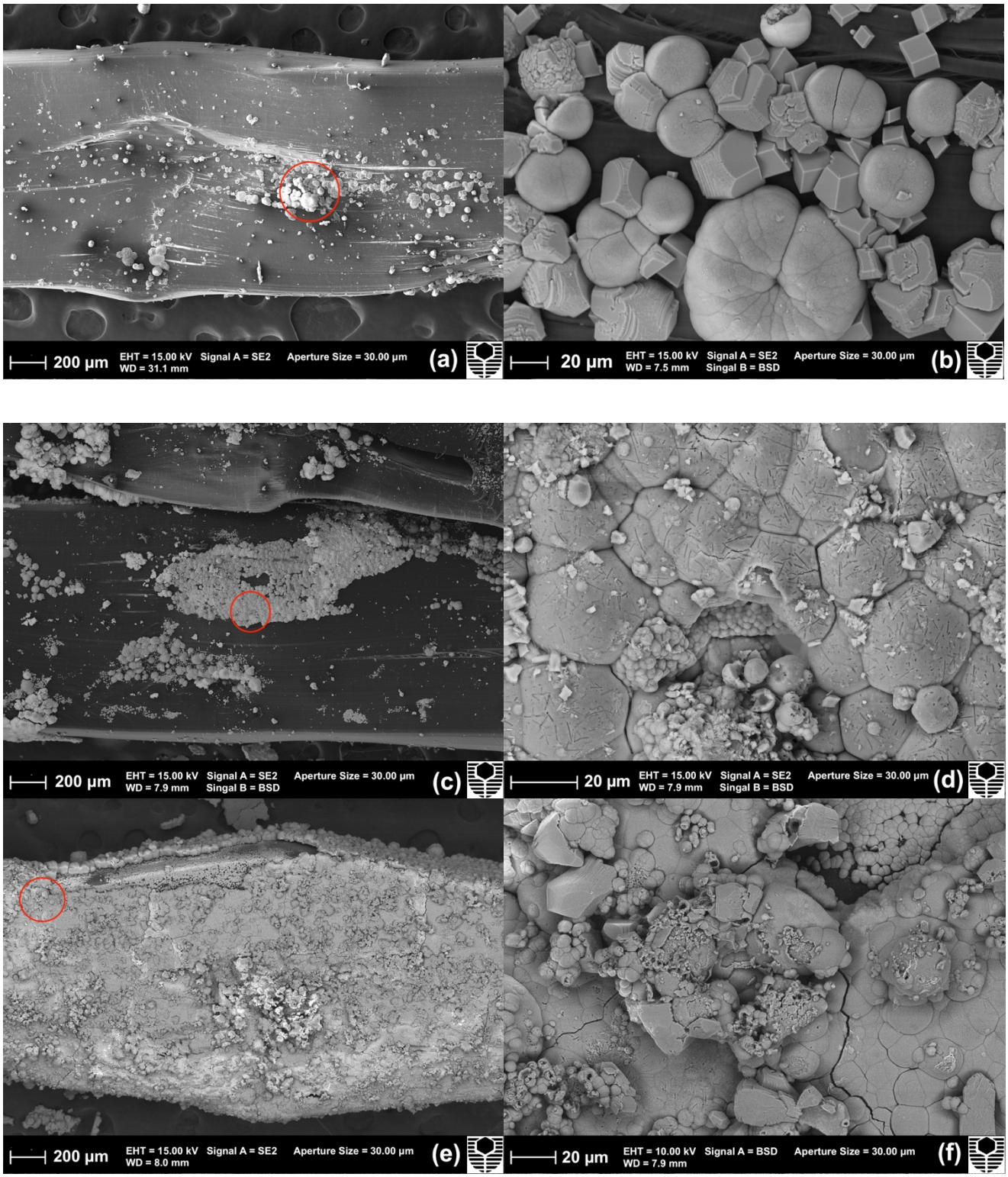
200 µm
EHT = 15.00 kV
WD = 31.1 mm
Signal A = SE2
Aperture Size = 30.00 µm
(a)
20 µm
EHT = 15.00 kV
WD = 7.5 mm
Signal A = SE2
Singal B = BSD
Aperture Size = 30.00 µm
(b)
200 µm
EHT = 15.00 kV
WD = 7.9 mm
Signal A = SE2
Singal B = BSD
Aperture Size = 30.00 µm
(c)
20 µm
EHT = 15.00 kV
WD = 7.9 mm
Signal A = SE2
Singal B = BSD
Aperture Size = 30.00 µm
(d)
200 µm
EHT = 15.00 kV
WD = 8.0 mm
Signal A = SE2
Aperture Size = 30.00 µm
(e)
20 µm
EHT = 10.00 kV
WD = 7.9 mm
Signal A = BSD
Aperture Size = 30.00 µm
(f)

Figure 3

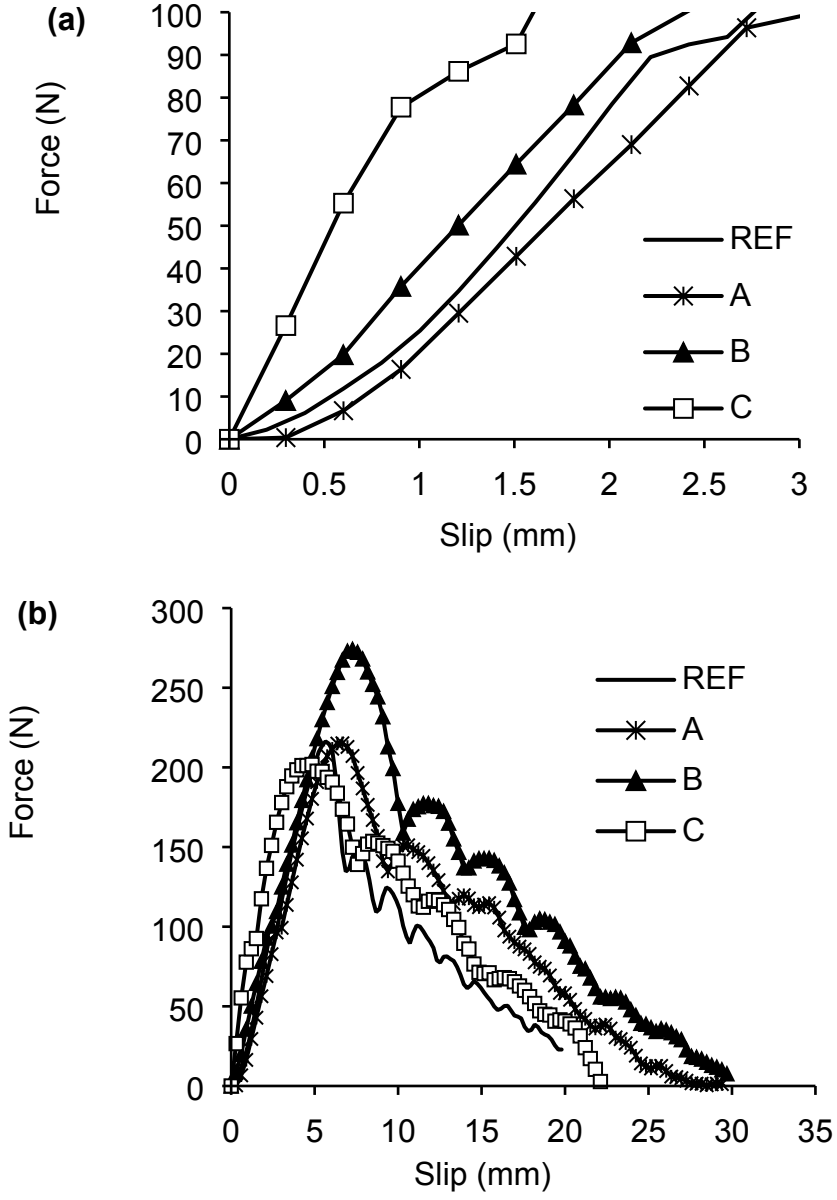
(a)
Force (N)
100
90
80
70
60
50
40
30
20
10
0
0
0.5
1
1.5
2
2.5
3
Slip (mm)
REF
A
B
C
(b)
Force (N)
300
250
200
150
100
50
0
0
5
10
15
20
25
30
35
Slip (mm)
REF
A
B
C

Figure 4

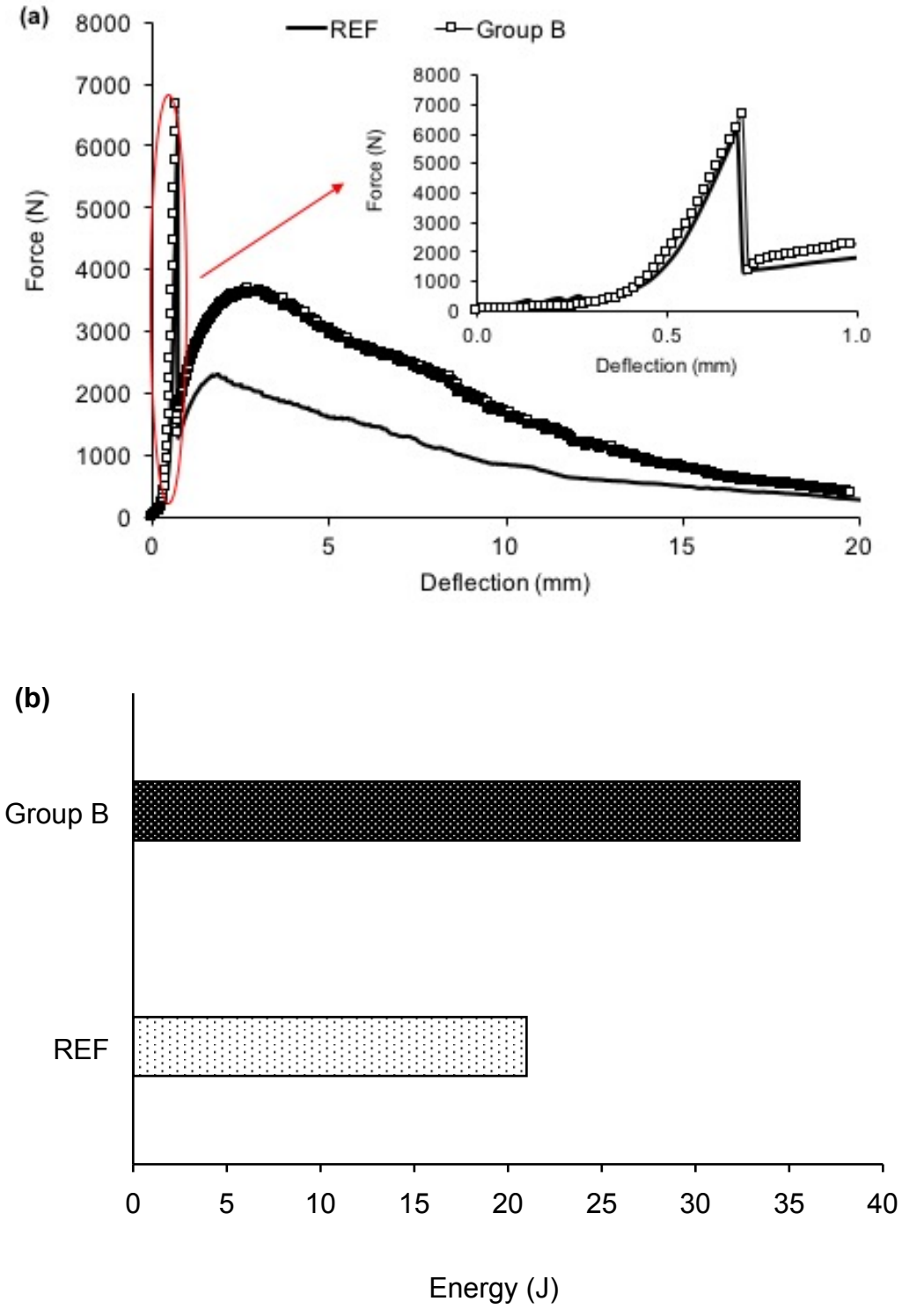

Figure 5

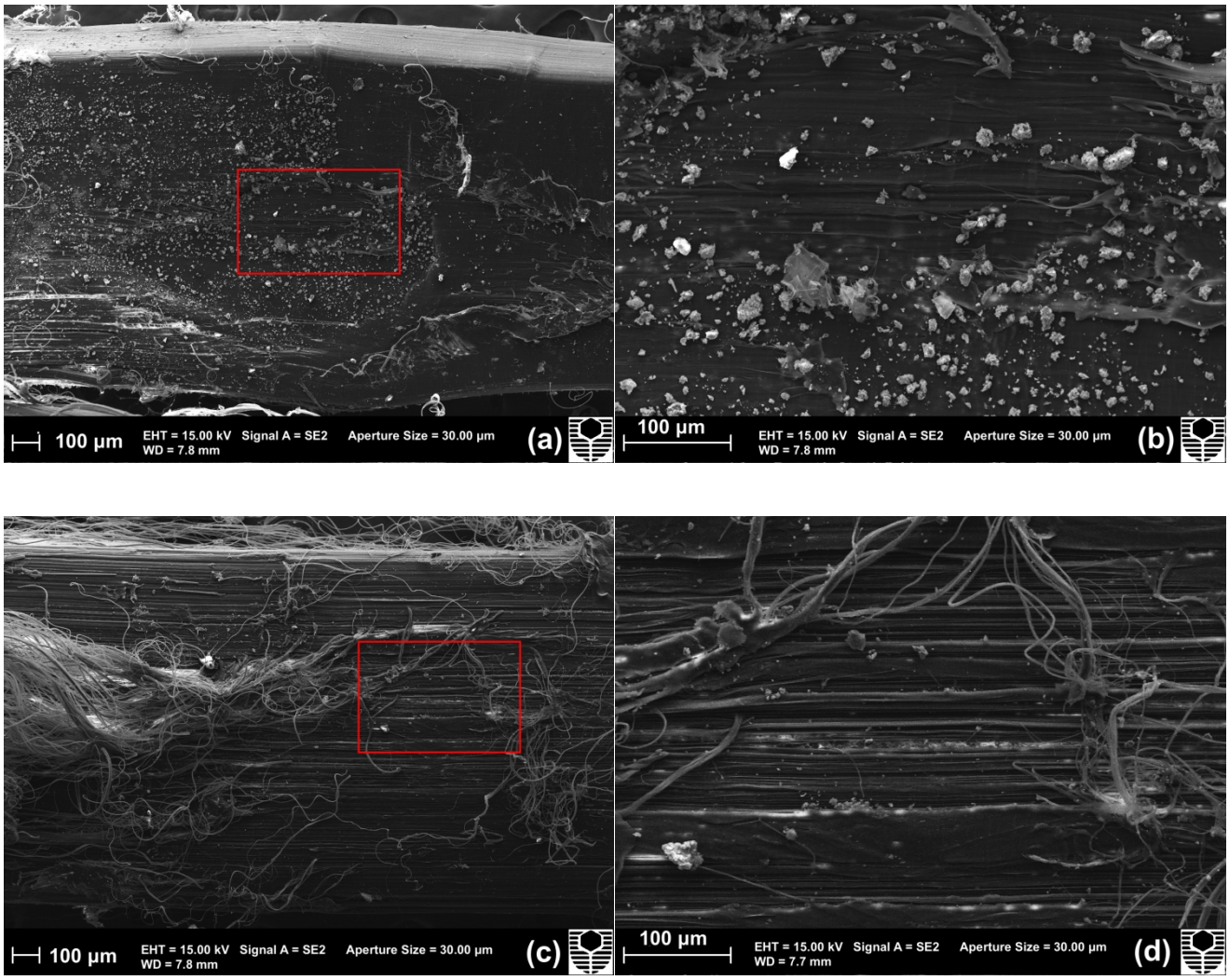
100 µm
EHT = 15.00 kV
WD = 7.8 mm
Signal A = SE2
Aperture Size = 30.00 µm
(a)
100 µm
EHT = 15.00 kV
WD = 7.8 mm
Signal A = SE2
Aperture Size = 30.00 µm
(b)
100 µm
EHT = 15.00 kV
WD = 7.8 mm
Signal A = SE2
Aperture Size = 30.00 µm
(c)
100 µm
EHT = 15.00 kV
WD = 7.7 mm
Signal A = SE2
Aperture Size = 30.00 µm
(d)

Figure 6

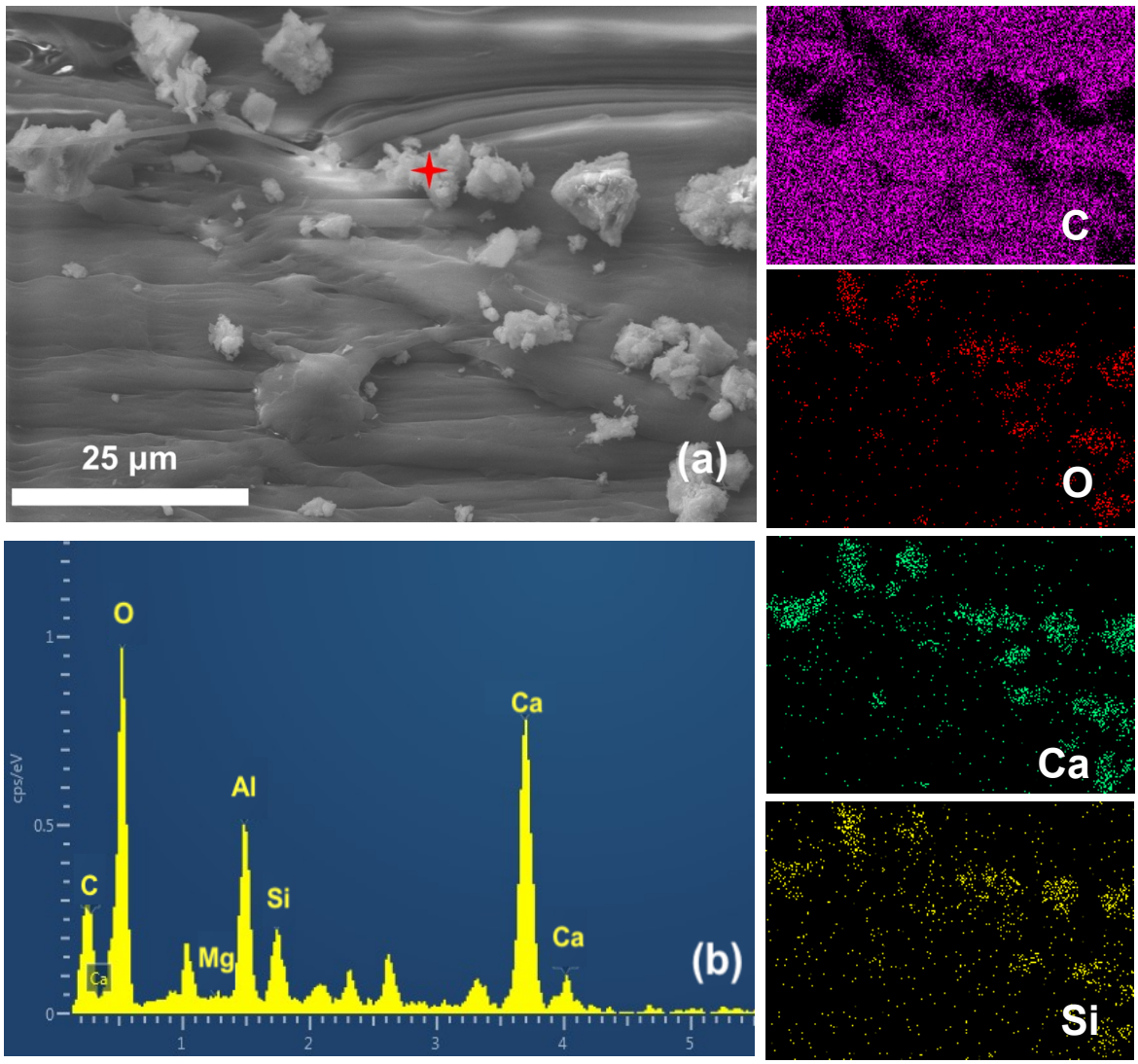

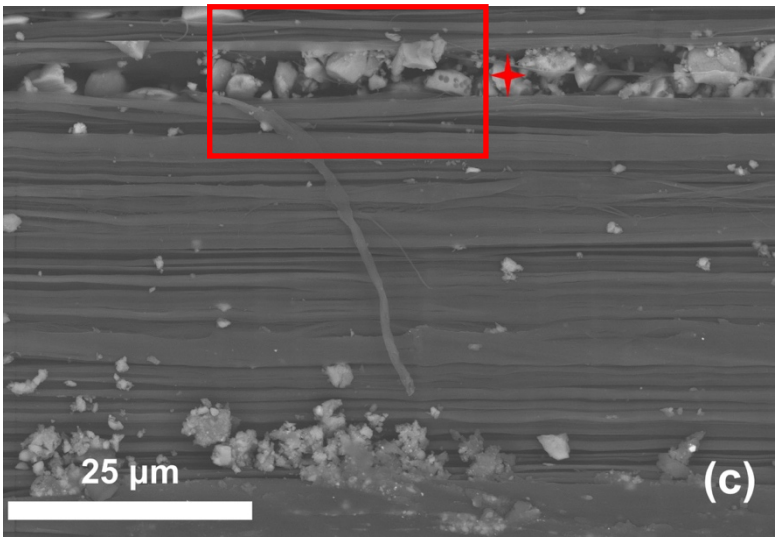
25 µm
(c)

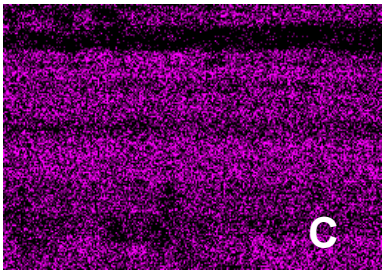
C

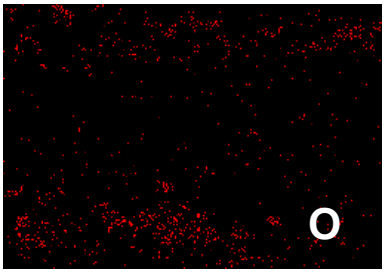
O

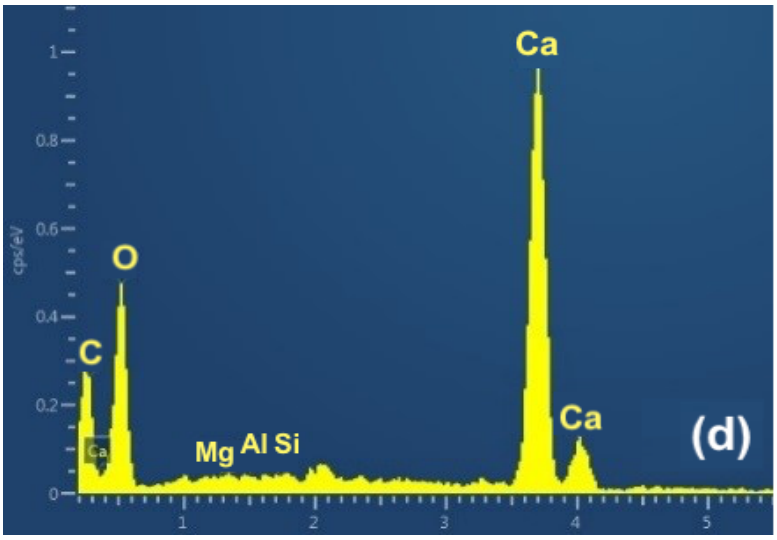
Ca
O
C
Mg Al Si
Ca
(d)
cps/eV
0
0.2
0.4
0.6
0.8
1
1
2
3
4
5

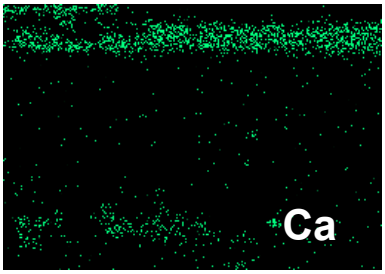
Ca

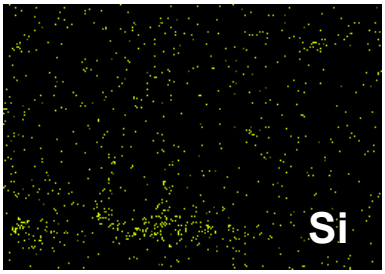
Si

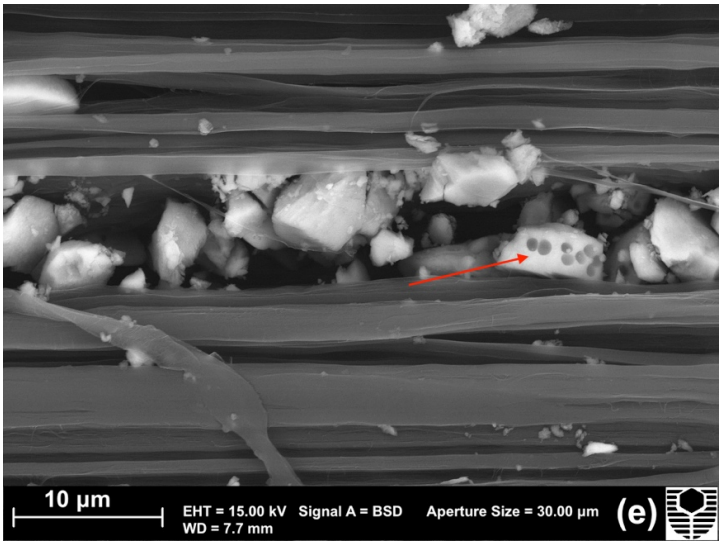
10 µm
EHT = 15.00 kV
WD = 7.7 mm
Signal A = BSD
Aperture Size = 30.00 µm
(e)